10.1109/ULTSYM.2011.0184

3D Direction of Arrival Estimation and Localization Using Ultrasonic Sensors in an Anechoic Chamber

Vitaliy Kunin, Weidi Jia, Marcos Turqueti, Jafar Saniie and Erdal Oruklu

Department of Electrical and Computer Engineering
Illinois Institute of Technology
Chicago, Illinois, 60616

Abstract—**This paper presents the design of an acoustic sensor array for sound source localization and object detection. An FPGA based data acquisition system is developed for a flexible acoustic sensor array platform. An anechoic chamber is designed to create a clean environment which isolates the experiment from external noises and reverberation echoes. We investigate direction of arrival estimation and source localization experiments with different geometries and with different numbers of sensors. We further present a discussion of parameters that influence the sensitivity and accuracy of the results of these experiments.**

Keywords- sound source localization; ultrasound; acoustic arrays; MEMS; sound imaging; sound tracking

I. INTRODUCTION

Acoustic sensor arrays are used in important applications such as multi-party telecommunications, hands-free acoustic human-machine interfaces, computer games, dictation systems, hearing-aids, medical diagnostics, structural failure analysis of buildings or bridges, and mechanical failure analysis of machines such as vehicles or aircrafts, and robotic vision, navigation and automation[1-5]. In practice, there are a large number of issues encountered in the real world environment which make realistic application of the theory significantly more difficult [6-9].

This work emphasizes the design and development of sound and ultrasound localization systems. An introduction to commonly used terminology, concepts and mathematics is given. Real world application issues described above are addressed; this includes a presentation of how an anechoic chamber and acoustic arrays were used to create a controlled experimental setup in which noise, reverberation echoes, source distance and angles, number and geometry of sensors could be varied. In the following sections, we explain the sound localization techniques, introduce the proposed sensor platform and discuss the experimentation setups with the corresponding sound and ultrasound localization performance.

II. THE PARAMETER ESTIMATION PROCEDURE

Sound and ultrasound source localization is the process of determining the position of an acoustic source, such as a human speaker, a stereo system speaker, or an ultrasound transducer using two or more receivers or microphones. A similar but separate topic is direction of arrival estimation (DOAE) which only determines the direction of the sound source but not the distance to it [7]. Both localization and DOAE can be broken down into several types. One distinction that can be made is whether 2-dimensional (2D) source localization and DOAE or 3-dimensional (3D) localization and DOAE is being performed. This simply refers to only looking for a sound source in a plane, i.e. only horizontally or vertically, or in full 3D space. Another consideration of source localization is whether near-field or far-field modeling is being used [7,10]. Source localization can be performed by determining delays between the source's transmit time and receivers' pickup times, or delays between only the receivers' pickup times (known as TDOA).

In general, both localization and DOAE can be divided into three general steps: collecting data across multiple receivers and/or transmitters, finding the phase difference and/or time difference of arrival, and calculating the direction and possibly distance to the sound source.

III. DIRECTION OF ARRIVAL ESTIMATION

The geometry of 2D DOAE is illustrated in Figure 1a. In this figure a source transmitter (*Tx*) is emitting a signal. This signal will then propagate through the air toward the two receivers (Rx_1 and Rx_2). As can be seen from the figure, since the two receivers are at different distances from the source the signal will reach them at different times, this is referred to as the TDOA marked as *T*. Based on this TDOA, the direction of the source with respect to the receivers can be estimated.

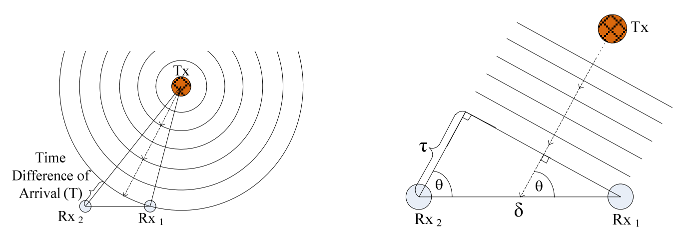

Fig. 1.a) 2D DOAE Geometry b) Far Field Model

The estimation of the direction of the source can then be obtained through the use of the far-field model [7]. The far-field model assumes that the receivers are far enough away from the source as to allow the spherical wave propagation shown in Figure 1a to be approximated by planes. This model is shown in Figure 1b.

In this model the angle that the source makes to the plane connecting the two receivers is given by θ, the distance between the receivers is δ, and the distance corresponding to the TDOA is τ. The TDOA is the information that is directly obtained from the receivers and τ is given by equation (1)

$$\tau = c\,T \tag{1}$$

where c is the speed of sound and T is the delay, in seconds between the two received signals. The inter-receiver distance is typically known since it can be set or measured by the designer or user. From this model, it can be seen that the angle of the direction of the source to the receivers can be related to T and δ by equation (2) given below.

$$\tau = \delta \cos(\theta) \tag{2}$$

Thus equation (3) gives the direction of the source.

$$\theta = \cos^{-1}(\tau / \delta) = \cos^{-1}(c\,T / \delta) \tag{3}$$

IV. Localization

2D localization can be performed with 3 receivers using only the TDOA information. The geometry for 2D localization using three receivers can be divided into two groups: one where the receivers are arranged in a line and the other where the receivers are arranged in a plane. The basic geometry with the receivers arranged in a line is shown in Figure 2a) [7].

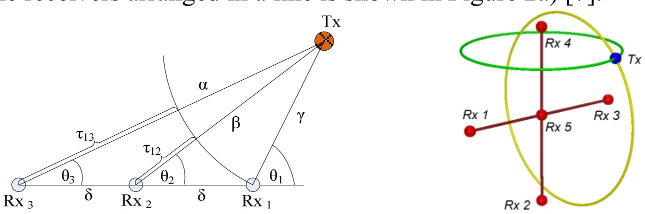

Fig. 2. a) 2D localization geometry b) 3D localization geometry

In this model θ_1, θ_2, and θ_3 are the angles from receivers 1, 2, and 3 to the source, respectively. α, β and γ are the distances from the source to receivers 1, 2, and 3, respectively. The distance between the receivers is δ. In this example, the two distances are made to be equal for simplicity. If they were different, the calculation would still work. The distances τ_{12} and τ_{13} are those corresponding to the TDOA between receivers 1 and 2, and between receivers 1 and 3, respectively, and are given by equations (4) and (5).

$$\tau_{12} = c\,T_{12} = \beta - \gamma \tag{4}$$

$$\tau_{13} = c\,T_{13} = \alpha - \gamma \tag{5}$$

Using the law of cosines equations (6) and (7) can be obtained to relate distances γ, α, β, δ and angle θ_1.

$$\beta^2 = \gamma^2 + \delta^2 + 2\,\gamma\,\delta \cos(\theta_1) \tag{6}$$

$$\alpha^2 = \gamma^2 + (2\delta)^2 + 4\,\gamma\,\delta \cos(\theta_1) \tag{7}$$

Equations (4) and (5) can then be substituted into equations (6) and (7) to give equations (8) and (9).

$$(c\,T_{12} + \gamma)^2 = \gamma^2 + \delta^2 + 2\,\gamma\,\delta \cos(\theta_1) \tag{8}$$

$$(c\,T_{13} + \gamma)^2 = \gamma^2 + (2\,\delta)^2 + 4\,\gamma\,\delta \cos(\theta_1) \tag{9}$$

Equations (8) and (9) are two equations in two unknowns since the T_{12} and the T_{13} will be the collected data and δ as well as c are known quantities. Using equations (8) and (9) the variables γ and θ_1 can be solved for. Next equations (4) and (5) can be used to solve for β and α. Now applying the cosine rule to triangle γ, δ, β gives angle θ_2 and applying the cosine rule to triangle β, δ, α gives angles θ_3. Thus, the distance and angle from each receiver can be obtained.

3D localization can be decomposed into two problems of 2D localizations as shown in Figure 2b). Here three receivers in each plane are used in the same way that they were used for 2D localization, with both results using the same coordinate system centered at receiver 5. Since two planes are used all information about the source is obtained. Geometrically, this is the same as finding two circles, or semi-circles, the intersection of which is the location of the sound source.

V. Microphone Array and Anechoic Chamber

The MEMS Array acouStic Imaging (MASI) used in this work is a novel PC/FPGA based data acquisition system with an embedded MEMS based microphone array (see Figure 3). The data acquisition system is flexible, expandable, scalable, and has both logging and real-time signal processing capability. More specifically, the system can collect data from 52 omnidirectional microphones simultaneously at sampling rates up to 300 Ksps. This data can be processed in real-time using the FPGA and then sent to a PC or alternatively the raw unprocessed data can be sent to a PC. The system to PC communications is performed through a gigabit Ethernet connection allowing high rates of transfer for the massive amount of data.

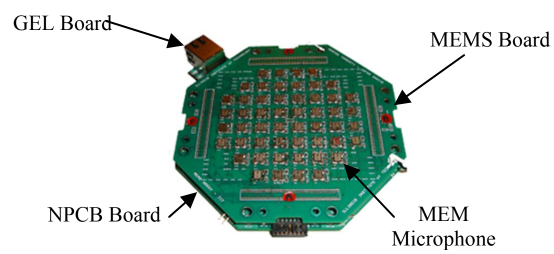

Fig. 3. MEMS Array acouStic Imaging (MASI)

To create a controlled environment for acoustic experimentation a 52”x52”x27” anechoic chamber was designed and built in order to isolate the experiment inside the chamber from outside noise and to absorb sound inside the chamber to prevent multiple reflections (aka, reverberation). The foam used for sound absorption was high density 2” thick polyester-based polyurethane convoluted foam which is specifically designed for sound absorption. Figure 4a) shows the outside view of the assembled anechoic chamber. In order to conduct a wide variety of acoustic and ultrasound experiments a sensor array test stand was designed and built. Figure 4b) shows a picture of the sensor array test stand which is made of a sensor bed and a stand. The sensor bed is 9.45”x11”, made from 2” foam attached to a wooden backbone. Foam is used to reduce reflections and noise vibrations coupling. The sensor bed contains 25 sensor positions arranged in a 5x5 square layout.

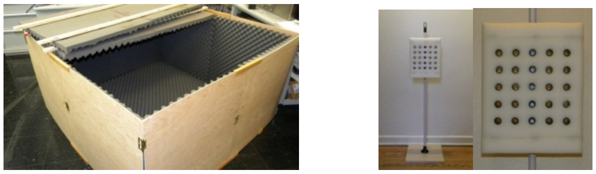

Fig. 4. a) Anechoic Chamber b) Sensor Array Test Stand

VI. Direction of Arrival Estimation Experiments

A variety of phase based sound source DOAE experiments were performed. The direction of the sound source was calculated based on the recorded phase delay and the distance between the receiving microphones. The first set of experiments involved the MASI, FPGA based microphone array data acquisition system, and a transmitting speaker. The microphone array data acquisition system was mounted on vise base, the transmitting speaker was also mounted on a vise base. The parameters varied in this experiment were the distance to the sound source, frequency of the sound source, the pairs of microphones used, and the angle between the sound source and the microphones. For the first test, the distance between the receivers and transmitter was two feet and for the second test the distance was 5 inches. The sound source signal used was a continuous sine wave of frequencies 1 kHz and 2 kHz, generated by an arbitrary waveform generator. The distance between the set of receivers was 2.75”. The upper frequency was limited to 2 kHz to allow all microphones of the microphone array system to be used without aliasing.

A. DOAE Experiment Set 1 using MEMs array

The results of this set of experiments are shown in Table 1. Here the angle of the sound source to the microphones is shown in the first column, the measurements for the two distances at two frequencies are shown in the second, third and fourth columns and the expected values are shown in the fifth column.

Table I. DOAE Experiment Set 1 Results

	Outer Microphones				
	Obtained Delay (ms)				Theoretical (Expected) Delay (ms)
Angle (°)	2' Distance		5" Distance		
	1 kHz	2 kHz	1 kHz	2 kHz	
0	-0.007	0.011	0	0.005	0
10	0.020	0.087	0.036	0.032	0.035
20	0.120	0.062	0.065	0.063	0.070
30	0.065	0.087	0.099	0.109	0.101
40	0.113	0.163	0.124	0.119	0.130
50	0.182	0.054	0.144	0.128	0.156
60	0.146	0.123	0.179	0.145	0.176
70	0.187	0.183	0.185	0.188	0.191
80	0.192	0.188	0.202	0.197	0.200

It can be seen from these results that phase based DOAE in a highly noisy and reverberant environment does not produce reliable results at larger distances independent of the frequency of the source signal or the distance between the receiving microphones. In the following sections, we introduce several practical steps to address these issues and improve the sound localization.

B. DOAE Experiment Set 2 using Anechoic Chamber:

In order to reduce the effect of reflection and ambient noise the second set of experiments were carried out inside the anechoic chamber. The results of this set of experiments are shown in Table II below.

Table II. DOAE Experiment Set 2 Results

	Outer Microphones				
	Obtained Delay (ms)				Theoretical (Expected) Delay (ms)
Angle (°)	2' Distance		5" Distance		
	1 kHz	2 kHz	1 kHz	2 kHz	
0	0.003	-0.005	0	0	0
10	0.015	0.012	0.034	0.035	0.035
20	0.045	0.040	0.068	0.069	0.070
30	0.064	0.077	0.102	0.101	0.101
40	0.060	0.064	0.131	0.132	0.130
50	0.067	0.071	0.153	0.157	0.156
60	0.130	0.121	0.176	0.178	0.176
70	0.180	0.176	0.193	0.189	0.191
80	0.190	0.193	0.199	0.201	0.200

From these results it can be seen that performing phase based sound source DOAE inside an acoustic chamber, which absorbs sound and thus reduces reflections, produces some improvement. However it can also be seen that the collected data still does not match the expected results thus there are still some reflections present in the environment.

C. DOAE Experiment Set 3 with modified receiver physical assembly

In order to reduce the effect of the reflection from the microphone array itself, an alternate physical setup and acquisition system was used for the third set of experiments. The physical setup consisted of a vise with generic 60° beam angle microphone attached to each of the two arms of the vise through foam with nothing in between the vise arms, the distance between the microphones was increased to 6.3”. To comply with the spatial sampling theorem given in equation 10, the frequency of the source signals was changed to 700 Hz and 900 Hz to work with the greater distance between the receivers. The results are shown in Table III.

Table III. Sound Source DOAE Experiment Set 3 Results

Angle (°)	Obtained Delay (ms) Frequency 700 Hz	Obtained Delay (ms) Frequency 900 Hz	Theoretical (Expected) Delay (ms)
0	0	0	0
10	0.061	0.084	0.081
20	0.112	0.146	0.160
30	0.156	0.215	0.234
40	0.209	0.292	0.301
50	0.244	0.340	0.359
60	0.295	0.391	0.407
70	0.317	0.446	0.442
80	0.344	0.452	0.463

It can be observed that increasing the distance between the microphones and removing any reflective surfaces from in between the microphones significantly improves the accuracy of phase based DOAE even at larger distances.

D. DOAE Experiment Set 4 using shortened transmission signal

This time instead of using a continuous sine wave for the source signal only a 20 cycle sine wave was transmitted. Then, when this sine pulse train wave was received, only the first pulse was used for phase comparison. This was expected to further reduce errors due to reflections since the first pulse should arrive before all reflections and thus its phase information should not be distorted. The results of this set of experiments are shown in Table IV below.

Table IV. Sound Source DOAE Experiment Set 4 Results

Angle (°)	Obtained Delay (ms) Frequency 700 Hz	Obtained Delay (ms) Frequency 900 Hz	Theoretical (Expected) Delay (ms)
0	0.010	0.015	0
10	0.092	0.092	0.081
20	0.175	0.180	0.160
30	0.250	0.254	0.234
40	0.310	0.320	0.301
50	0.360	0.356	0.359
60	0.405	0.412	0.407
70	0.440	0.442	0.442
80	0.465	0.462	0.463

From these results it can be observed that phase based DOAE which uses the phase information from only the first wave pulse provides accurate results even at larger distances and independent of the frequency of the source signal.

VII. Ultrasound Localization Experiments

Higher accuracy measurements can be achieved using higher sound frequencies and narrower beamfields for both transmitter and receiver. To demonstrate this, two types of ultrasound source localization experiments were performed. The first was a 2D ultrasound source localization experiment and the second was a 3D ultrasound source localization experiment. Both of the experiments were carried out inside the anechoic chamber. The first experiment consisted of three 40 kHz ultrasound transducers which acted as receivers and one 40 kHz omnidirectional ultrasound transmitter. The transmitter used a 20 cycle sine wave pulse train. The geometry and dimensions of the setup are shown in Figure 5a.

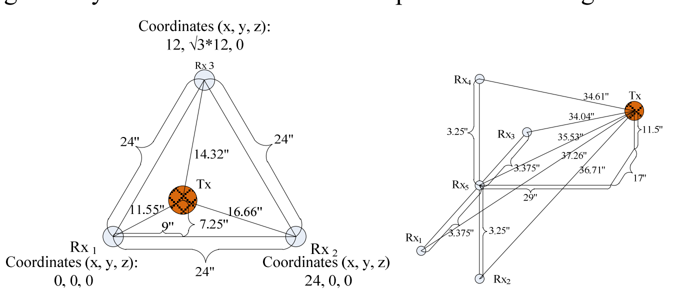

Fig. 5. a) 2D Localization b) 3D Localization

In Figure 5a, the transmitter is labeled *Tx*, and the receivers are labeled Rx_1 through Rx_3. The results of this set of experiments are shown in Table V. The second experiment consisted of six 40 kHz ultrasound transducers, five of which acted as receivers and one of which acted as a transmitter. The transmitter used a 20 cycle sine wave pulse train. The sensor array test stand as was used to hold the transmitter and receivers. The geometry and dimensions of the setup are shown in Figure 5b. The results of this set of experiments are shown in Table VI.

Table V. Experimental Results: 2D Distances

From Receiver	Collected (inches)	Expected (inches)	Error (inches)
1	12.46	11.55	0.91
2	17.41	16.66	0.75
3	14.69	14.32	0.37

Table VI. Experimental Results: 3D Distances

From Receiver	Collected (inches)	Expected (inches)	Error (inches)
1	37.921	37.26	0.661
2	37.378	36.71	0.668
3	34.807	34.04	0.767
4	35.213	34.61	0.603
5	36.567	35.53	1.037

Both sets of experiments produce accurate ultrasound localization results and collected values are within a few percent of each other.

VIII. Conclusion

From this work it can be seen that parameters that affected the accuracy were the distance between the receivers and transmitter, the distance between the receivers, presence of reflective surfaces close to the receivers, and the frequency of the source signal. Ultrasound localization experiments showed better accuracy and less susceptibility to noise and reflections. The estimation techniques used in this work could be important for applications such as robotic auditory systems, voice based man-machine interfacing and ultrasound beacon based object tracking.

References

[1] H. Alghassi, "Eye Array Sound Source Localization," Doctoral dissertation, University of British Columbia, Vancouver, 2008.

[2] J. Eckert, R. German, and F. Dressler, "An Indoor Localization Framework for Four-Rotor Flying Robots Using Low-Power Sensor Nodes," *Instrumentation and Measurement, IEEE Transactions on,* Vol. 60, No. 2, 2011, pp. 336-344.

[3] S. Harput, and A. Buzkurt, "Ultrasonic Phased Array Device for Acoustic Imaging in Air," *IEEE Sensors Journal*, Vol. 8, No. 11, 2008, pp. 1755-1762.

[4] S. J. Kim, and B. K. Kim, "Accurate Hybrid Global Self-Localization Algorithm for Indoor Mobile Robots with Two-Dimensional Isotropic Ultrasonic Receivers," *Instrumentation and Measurement, IEEE Transactions on,* Vol. 99, 2011, pp.1-14,.

[5] J. R. Llata, E. G. Sarabia, and J. P. Oria, "Three Dimensional Robotic Vision Using Ultrasonic Sensors," *Journal of Intelligent and Robotic Systems, Berlin Heidelberg: Spring-Verlag.,* Vol. 33, No. 3, 2002, pp. 267-284.

[6] B. Shaw, "Source Localization and Beamforming," *IEEE Signal Processing Magazine*, Vol. 19, No. 2, 2002.

[7] J. Benesty, J. Chen, and Y. Huang, "Microphone Array Signal Processing," Berlin Heidelberg: Spring-Verlag. 2008.

[8] M. Brandstein and D. Ward, (Eds.), "Microphone Arrays Signal Processing Techniques and Applications," Berlin Heidelberg: Spring-Verlag, 2001.

[9] V. D. Rabinkin, J. R. Renomeron, C. J. French, and L. J. Flanagan, "Estimation of Wavefront Arrival Delay Using the Cross-Power Spectrum Phase Technique," *132nd meeting of the Acoustic Society of America*, Honolulu, HI. 1996.

[10] I. McCowan, "Microphone Arrays: A tutorial," Doctoral dissertation, Queensland University of Technology, Australia, 2001.